ELSEVIER

PALAEO

Palaeogeography, Palaeoclimatology, Palaeoecology 162 (2000) 211–223

www.elsevier.nl/locate/palaeo

A global carbon isotope excursion (SPICE) during the Late Cambrian: relation to trilobite extinctions, organic-matter burial and sea level

Matthew R. Saltzman [a,*], Robert L. Ripperdan [b], M.D. Brasier [c], Kyger C. Lohmann [d], Richard A. Robison [e], W.T. Chang [f], Shanchi Peng [f], E.K. Ergaliev [g], Bruce Runnegar [h]

[a] *Department of Geological Sciences, The Ohio State University, Columbus, OH 43210, USA*
[b] *Department of Geology, University of Puerto Rico, Mayaguez 00681-5000, Puerto Rico*
[c] *Department of Earth Sciences, University of Oxford, Oxford OX1 3PR, UK*
[d] *Department of Geological Sciences, University of Michigan, Ann Arbor, MI 48109-1063, USA*
[e] *Department of Geology, University of Kansas Lawrence, KS 66045, USA*
[f] *Nanjing Institute of Geology and Palaeontology, Academia Sinica, Nanjing 210008, People's Republic of China*
[g] *Institute of Geological Sciences, 480100 Almaty, Kazakhstan*
[h] *Department of Earth and Space Sciences and Institute of Geophysics and Planetary Physics, University of California, Los Angeles, CA 90095-1567, USA*

Received 28 September 1999; accepted for publication 25 April 2000

Abstract

The Steptoean positive carbon isotope excursion (SPICE) marks a global oceanographic event that confirms intercontinental correlations between different biogeographic realms based on agnostids and other blue-water trilobites. The SPICE excursion is documented from sections in Laurentia, Kazakhstan, China, and Australia where it begins with the mass extinction at the base of the Pterocephaliid Biomere (Steptoean Stage) in Laurentia and at coeval extinction horizons in Gondwana and periGondwana terranes. The peak of SPICE (+5‰) coincided with a time of maximum regression in Laurentia. SPICE is similar in this regard to excursions that coincide with glacio-eustatic falls, such as in the Late Ordovician. A plausible scenario involves the transformation of ocean circulation between two states, which led to enhanced coastal upwelling and benthic extinctions. The lack of evidence for glaciation indicates that the coeval sea level fall (Sauk II–Sauk III event) resulted from tectonic or hydrologic changes that remain poorly understood at this time.

Keywords: biomere; carbon-isotopes; mass extinction; Upper Cambrian

* Corresponding author.
E-mail address: saltzman@geology.ohio-state.edu (M.R. Saltzman)

0031-0182/00/$ - see front matter © 2000 Elsevier Science B.V. All rights reserved.
PII: S0031-0182(00)00128-0

1. Introduction

Carbon isotope ratios of marine limestones hover ca. 1–2‰ above the PDB standard value of $\delta^{13}C = 0$‰ for much of the Phanerozoic. Intervals of significantly positive carbon isotope ratios ($\geq +2$‰) are thought to coincide with times of increased burial of organic matter, either in coal basins (Carboniferous and Permian) or as marine petroleum source rocks (Jurassic and Cretaceous). Short-lived positive carbon isotope excursions may peak at even heavier isotope ratios ($\geq +5$‰), presumably because the processes that caused them cannot be sustained for tens of millions of years. Several of these extraordinary positive events are known to be associated with mass extinctions of marine invertebrates. These include the Cenomanian–Turonian (C–T, Scholle and Arthur, 1980; Arthur et al., 1987; Jenkyns et al., 1994), Frasnian–Famennian (Joachimski and Buggisch, 1993; Wang et al., 1996), and end-Ordovician (Brenchley et al., 1994; Underwood et al., 1997; Kump et al., 1999) extinction events.

Here, we document a large and global positive excursion in $\delta^{13}C$ of Late Cambrian carbonates from North America (Laurentia), Kazakhstan, South China and Australia (Gondwana) that begins at a worldwide extinction of trilobites first identified in North China by Charles D. Walcott (1913). This Steptoean positive carbon isotope excursion (SPICE) represents a major perturbation of the Cambrian carbon cycle (Saltzman et al., 1998) that lies midway (~500 Ma) between comparable end-Proterozoic (549 Ma; Grotzinger et al., 1995) and end-Ordovician (~446 Ma; Underwood et al., 1997; Tucker and McKerrow, 1995) phenomena. The distinguishing feature of the SPICE excursion is that the accompanying extinction coincides with the onset of the positive shift, rather than with the rising limb of the excursion. In fact, peak faunal diversity correlates with the peak of the SPICE excursion in North America (Rowell and Brady, 1976). Thus, in contrast to the C–T extinction event, this Upper Cambrian faunal crisis appears to have resulted from the cause of the carbon cycle perturbation (e.g. upwelling) rather than a deterioration of oceanic conditions which may have developed during the SPICE excursion. An explanation that accounts for both the mass extinction and the SPICE excursion must therefore involve a process which began swiftly and then continued to operate on a multimillion year time scale (Saltzman et al., 1998).

2. Litho- and biostratigraphy of sampled sections

Carbonates analyzed for carbon isotopic ratios come from two separate passive continental margins of Late Cambrian (~500 Ma) age (Fig. 1). The Wa'Ergang and Paibi sections, northwestern Hunan, China (Peng, 1992); and the Shingle Pass section, Nevada (Saltzman et al., 1998). In addition, sections were analyzed from an intracratonic basin: the GSQ Mt. Whelan 1 core in Queensland, Australia (Green and Balfe, 1980), and a section on the flanks of a seamount: the Kyrshabakty River section, Malyi Karatau region, Kazakhstan (Ergaliev, 1981; Cook et al., 1991).

2.1. Malyi Karatau region, Kazakhstan

Upper Cambrian carbonates sampled for $\delta^{13}C$ in Kazakhstan were deposited adjacent to (or on the flanks of) a seamount that formed over a structural high (Cook et al., 1991). Deep water carbonate deposition occurred in structural lows on the flanks. At the Kyrshabakty River section, carbonates were deposited in a submarine-fan environment adjacent to the Aisha Bibi seamount. The section (Fig. 2; Table 2) consists of varying proportions of fine-grained, dark-colored, argillaceous limestone and carbonate gravity-flow deposits. Cook et al. (1991) interpreted the upward-shallowing carbonate sequence in terms of a seaward-prograding platform margin and submarine fan. The oldest sampled Middle Cambrian sediments include basin-plain facies, which are overlain by outer fan and mid-fan distributary channel deposits. Inner fan and upper slope facies are ultimately capped by uppermost Cambrian shallow water seamount margin and interior facies consisting of *Epiphyton* bioherms. Numerous submarine slides, consisting of lithified segments of the seamount margin, occur throughout the Middle and Upper Cambrian sequence, with a particularly prominent

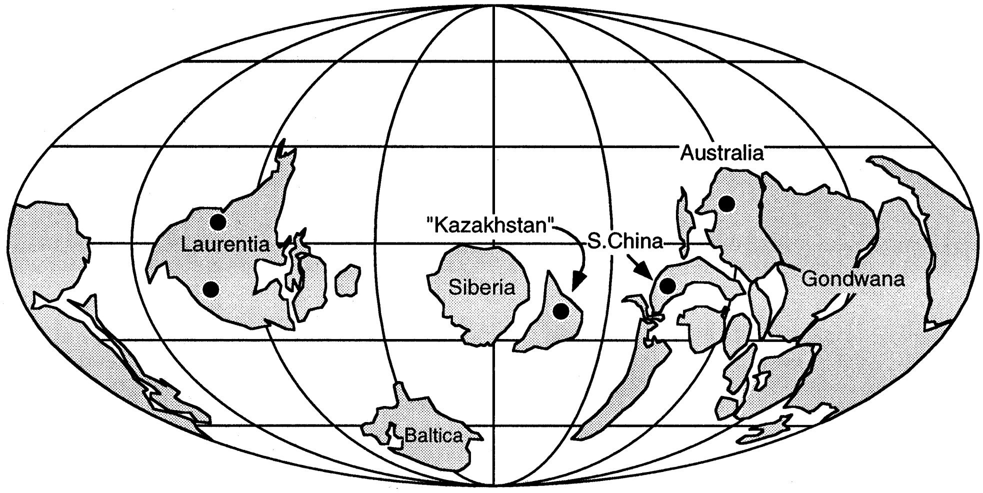

Fig. 1. Paleogeographic map for the Late Cambrian (after Scotese and McKerrow, 1990) showing approximate locations of the regions sampled. The SPICE excursion is also known from Tennessee (Glumac and Walker, 1998).

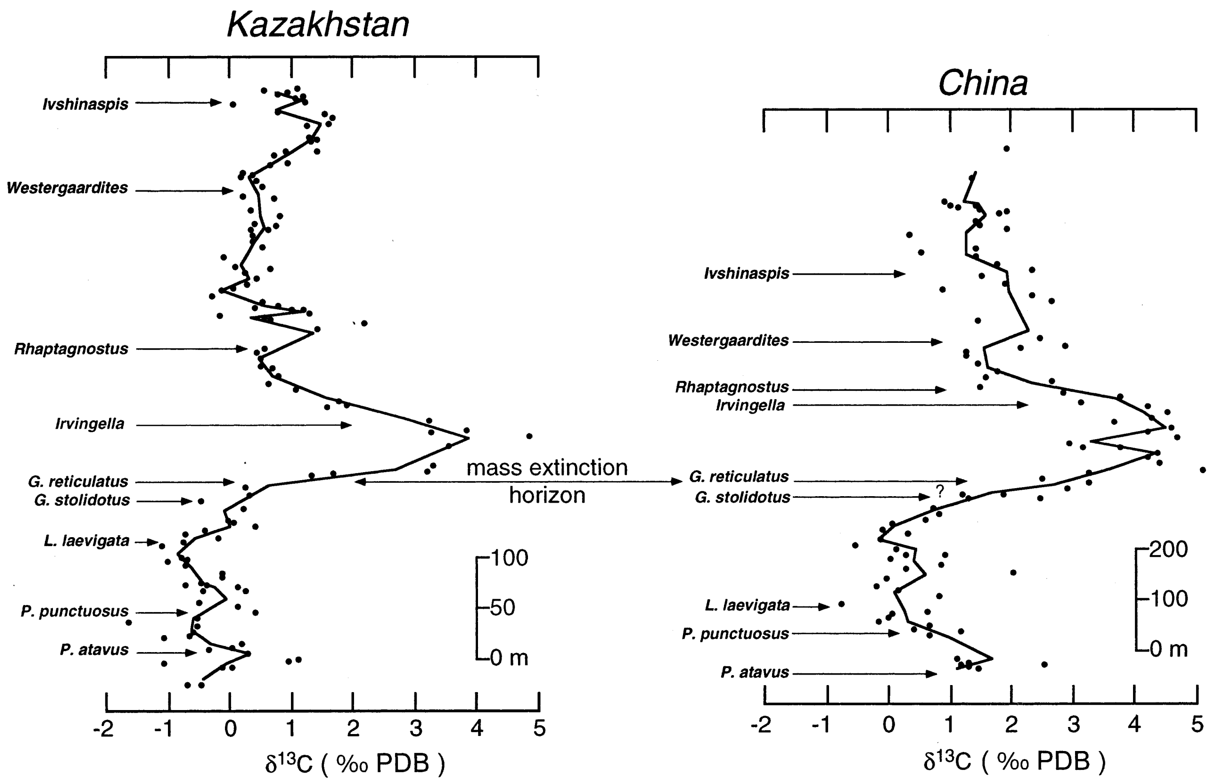

Fig. 2. Plots of $\delta^{13}C$ (‰) of limestones from the Wa'ergang and Paibi sections in Hunan, China (Peng, 1992) and the Kyrshabakty River section, Kazakhstan (Ergaliev, 1981). First occurrences of cosmopolitan trilobite taxa are shown. Data presented in Tables 1–3.

slide at the boundary between the Sackian and Malykaratauian Stages of Ergaliev (1981).

The biostratigraphy of the Kyrshabakty River section has been summarized by Ergaliev (1981). The documentation of faunal zones and our sampling for carbon isotopes starts in the *Ptychagnostus atavus* Zone. Key fossil occurrences representative of the overlying zones and useful in correlation with sections in China are plotted in Fig. 2 (*G. stolidotus* and *G. reticulatus*) and listed in Table 1 (also see Peng, 1992).

2.2. Northwestern Hunan, China

The Wa'Ergang and Paibi sections are situated within the Jiangnan Slope Belt, which represents

Table 1
Stable Isotope Data, Kazakstan

Meters	^{13}C	^{18}O	Zone	Meters	?^{13}C	?^{18}O	Zone	Meters	^{13}C	^{18}O	Zone
0.00	−0.73	−6.38	?	180.00	−0.51	−7.32	*G. stolidotus*	409.00	0.64	−7.71	*E. kazachstanicus*
0.10	−0.50	−6.23	?	186.00	0.29	−7.45	*G. stolidotus*	411.50	0.06	−7.18	*E. kazachstanicus*
16.00	−0.15	−7.16	?	194.00	0.22	−6.86	*G. stolidotus*	420.00	−0.13	−7.61	*E. kazachstanicus*
16.70	−0.01	−6.65	?	205.00	1.31	−7.13	*G. reticulatus*	431.00	0.50	−8.15	*E. kazachstanicus*
19.80	−1.11	−7.05	?	207.00	1.64	−6.48	*G. reticulatus*	437.00	0.34	−8.12	*E. kazachstanicus*
23.00	0.91	−6.43	?	209.50	3.17	−6.70	*I. inexpectans*	442.00	0.36	−8.37	*E. ovaliformis*
25.20	1.08	−7.40	?	215.50	3.28	−6.45	*I. inexpectans*	447.00	0.60	−7.81	*E. ovaliformis*
30.70	0.26	−7.84	?	235.00	3.51	−6.60	*A. acutatus*	448.00	0.33	−8.30	*E. ovaliformis*
33.50	−0.38	−7.60	*P. atavus*	243.50	4.82	−6.99	*A. acutatus*	452.00	0.74	−7.83	*E. ovaliformis*
35.30	−0.01	−7.95	*P. atavus*	248.00	3.24	−7.19	*A. acutatus*	453.00	0.37	−7.87	*E. ovaliformis*
39.50	0.17	−7.61	*P. atavus*	250.00	3.81	−7.09	*A. acutatus*	462.00	0.79	−7.62	*E. ovaliformis*
45.00	−1.11	−7.50	*P. atavus*	260.00	3.19	−6.96	*A. acutatus*	467.00	0.33	−8.87	*E. ovaliformis*
48.00	−0.70	−7.50	*P. atavus*	272.00	1.55	−6.59	*A. acutatus*	478.00	0.69	−7.54	*E. ovaliformis*
52.00	−0.64	−6.69	*P. atavus*	274.50	1.88	−8.59	*A. acutatus*	480.00	0.19	−10.19	*E. ovaliformis*
57.00	−0.56	−7.55	*P. atavus*	278.50	1.75	−8.85	*A. acutatus*	490.00	0.50	−7.79	*E. ovaliformis*
61.00	−1.69	−8.33	*P. atavus*	290.50	1.05	−7.06	*I. ivshini*	496.00	0.42	−7.89	*E. ovaliformis*
64.00	−0.56	−7.21	*P. atavus*	296.00	0.62	−7.83	*I. ivshini*	499.00	0.16	−7.76	*E. ovaliformis*
71.00	0.40	−7.49	*P. punctuosus*	304.00	0.78	−7.21	*I. ivshini*	502.00	0.36	−7.81	*E. ovaliformis*
76.50	0.11	−6.46	*P. punctuosus*	311.00	0.67	−7.27	*I. ivshini*	504.00	0.21	−7.50	*E. ovaliformis*
81.00	−0.53	−9.15	*G. nathorsi*	314.00	0.47	−6.90	*I. ivshini*	510.50	0.64	−8.94	*A. scrobicularis*
91.00	0.23	−7.75	*G. nathorsi*	321.00	0.47	−7.27	*I. ivshini*	514.00	0.93	−7.61	*A. scrobicularis*
96.00	0.10	−7.11	*G. nathorsi*	327.00	0.43	−7.17	*I. ivshini*	521.00	0.69	−7.28	*A. scrobicularis*
98.50	−0.42	−7.66	*G. nathorsi*	330.00	0.55	−6.91	*P. psuedangustilobus*	524.00	1.39	−7.91	*A. scrobicularis*
91.00	−0.46	−7.24	*G. nathorsi*	350.00	1.41	−6.72	*P. psuedangustilobus*	525.50	0.88	−7.66	*A. scrobicularis*
97.00	−0.76	−7.40	*G. nathorsi*	355.00	2.15	−6.75	*P. psuedangustilobus*	535.00	1.29	−8.56	*A. scrobicularis*
99.00	−0.49	−7.12	*G. nathorsi*	359.00	0.65	−6.77	*P. psuedangustilobus*	536.00	1.40	−8.22	*A. scrobicularis*
105.00	−0.14	−7.18	*L. armata*	361.00	0.53	−6.98	*P. psuedangustilobus*	539.00	1.28	−7.95	*T. trisulcus*
109.00	−0.15	−6.86	*L. armata*	364.00	−0.19	−7.04	*P. psuedangustilobus*	549.00	1.23	−7.96	*T. trisulcus*
116.00	−0.74	−7.27	*L. armata*	365.00	1.27	−6.61	*P. psuedangustilobus*	552.00	1.58	−8.46	*T. trisulcus*
120.00	−1.03	−7.28	*L. armata*	368.00	1.19	−7.55	*P. psuedangustilobus*	557.00	1.64	−8.47	*T. trisulcus*
122.00	−0.71	−6.87	*L. armata*	369.00	0.98	−7.29	*P. psuedangustilobus*	561.00	1.51	−8.17	*T. trisulcus*
124.00	−0.81	−7.07	*L. armata*	370.00	0.38	−7.13	*E. kazachstanicus*	564.00	0.75	−8.29	*T. trisulcus*
136.00	−1.12	−6.99	*L. armata*	373.00	0.76	−7.68	*E. kazachstanicus*	570.00	0.03	−8.55	*T. trisulcus*
140.00	−0.78	−7.09	*L. laevigata*	376.00	0.51	−7.05	*E. kazachstanicus*	572.00	1.20	−7.48	*T. trisulcus*
143.00	−0.22	−6.80	*L. laevigata*	382.00	−0.30	−7.08	*E. kazachstanicus*	576.00	1.06	−7.77	*T. trisulcus*
147.00	−0.76	−7.14	*L. laevigata*	388.00	−0.14	−7.02	*E. kazachstanicus*	579.00	1.19	−8.15	*T. trisulcus*
152.00	−0.43	−6.86	*L. laevigata*	391.00	0.03	−7.28	*E. kazachstanicus*	581.00	0.75	−8.27	*T. trisulcus*
156.00	0.39	−7.37	*L. laevigata*	394.00	0.26	−7.22	*E. kazachstanicus*	583.00	0.92	−8.29	*T. trisulcus*
159.00	0.04	−7.26	*K. simplex*	399.00	0.42	−7.11	*E. kazachstanicus*	585.00	0.54	−8.31	*T. trisulcus*
162.00	−0.06	−7.07	*K. simplex*	405.00	0.22	−7.78	*E. kazachstanicus*	587.00	1.07	−8.10	*T. trisulcus*
172.00	0.21	−7.75	*K. simplex*								

a transitional facies belt between the shallow water carbonates of the Yangtze Platform and the deep basinal deposits of the Jiangnan Basin (Peng, 1992). The oldest strata sampled for carbon isotopes come from the uppermost Aoxi Formation at the Paibi section (Fig. 2; Table 2). The Aoxi Formation is composed of unfossiliferous laminated dolomites with interbedded black shales near the top which represent the deepest water deposits within the Jiangnan Slope Belt. The Aoxi Formation is overlain by the abundantly fossiliferous Huaqiao Formation. The Huaqiao Formation consists of rhythmically bedded argillaceous limestones and calcareous shales, with minor dolomitic limestone interbeds. Breccia beds occur throughout the formation and are composed of limestone clasts derived from the Yangtze Platform. These breccia beds have been interpreted as debris flows reflecting episodic slumping of the upper slope and platform margin (Peng, 1992). Breccia beds become more common upsection and thus it appears that sea level was falling during deposition of the Huaqiao Formation (Peng and Robison, 2000). At Paibi, the Huaqiao Formation is overlain by a sparsely fossiliferous massive dolomite, representing progradation of the Yangtze Platform out onto the Jiangnan Slope Belt. However, facies representative of the Jiangnan Slope Belt persist ~120 km to the northeast at the Wa'Ergang section (Table 3), where the Huaqiao is overlain by fossiliferous fine-grained, argillaceous limestones of the Bitao, Chefu and Shenjiwan Formations. The boundaries between the Bitao, Chefu and Shenjiwan Formations were historically chosen to coincide with important biostratigraphic boundaries rather than lithostratigraphic boundaries (Peng and Robison, 2000).

Table 2
Stable Isotope Data, Paibi, China

Meters	?^{13}C	?^{18}O	Formation	Zone
−3.00	0.57	−8.19	Aoxi	*P. atavus*
20.00	1.47	−10.20	Huaqiao	*P. atavus*
27.50	1.30	−9.16	Huaqiao	*P. atavus*
30.50	2.55	−6.46	Huaqiao	*P. atavus*
31.00	1.17	−9.55	Huaqiao	*P. atavus*
34.20	1.30	−9.16	Huaqiao	*P. atavus*
40.00	1.10	−9.88	Huaqiao	*P. atavus*
88.50	0.68	−7.72	Huaqiao	*P. atavus*
93.50	1.18	−7.66	Huaqiao	*P. punctuosus*
100.80	0.41	−8.45	Huaqiao	*P. punctuosus*
107.00	0.67	−7.78	Huaqiao	*P. punctuosus*
113.00	−0.16	−8.88	Huaqiao	*P. punctuosus*
121.40	−0.01	−8.76	Huaqiao	*P. punctuosus*
128.50	0.07	−8.57	Huaqiao	*P. punctuosus*
135.00	0.65	−8.84	Huaqiao	*P. punctuosus*
148.00	−0.76	−9.00	Huaqiao	*L. laevigata*
165.00	0.82	−8.25	Huaqiao	*L. laevigata*
177.00	0.17	−8.78	Huaqiao	*L. laevigata*
182.30	−0.19	−8.73	Huaqiao	*L. laevigata*
200.00	−0.04	−7.88	Huaqiao	*L. laevigata*
208.70	2.02	−8.63	Huaqiao	*L. laevigata*
218.90	0.30	−8.94	Huaqiao	*L. laevigata*
226.50	0.86	−9.03	Huaqiao	*L. laevigata*
236.00	0.03	−9.06	Huaqiao	*L. laevigata*
256.00	0.12	−7.92	Huaqiao	*L. laevigata*
246.00	0.28	−9.00	Huaqiao	*L. laevigata*
246.50	0.91	−8.53	Huaqiao	*L. laevigata*
256.00	0.12	−7.92	Huaqiao	*L. laevigata*
266.20	−0.53	−8.02	Huaqiao	*L. laevigata*
276.80	−0.13	−7.66	Huaqiao	*L. laevigata*
286.00	0.32	−8.60	Huaqiao	*L. laevigata*
296.20	−0.10	−9.41	Huaqiao	*L. laevigata*
306.10	0.06	−8.36	Chefu	*L. laevigata*
316.00	0.62	−7.28	Chefu	*L. laevigata*
326.30	0.82	−8.77	Chefu	*L. laevigata*
336.80	0.73	−7.96	Chefu	*L. laevigata*
356.00	1.31	−9.14	Chefu	*L. laevigata*
366.00	1.20	−6.81	Chefu	*G. stolidotus*

The biostratigraphy of the Wa'Ergang section has been studied by Peng (1992) and the agnostid biostratigraphy of the diverse and abundant faunas at Paibi has been documented by Peng and Robison (2000). Agnostid trilobites are widely distributed in Middle to Upper Cambrian sections worldwide and are particularly useful for intercontinental correlation. The lowest correlatable agnostid zone is the *Ptychagnostus atavus* Zone, which occurs at the base of the Huaqiao Formation in both the Wa'Ergang and Paibi sections (Fig. 2; Tables 2 and 3). The first occurrence of *P. atavus* represents a globally recognized chronostratigraphic horizon within the Middle Cambrian (Rowell et al., 1982). Younger zones include the *Lejopyge armata* Zone at Wa'Ergang and the *Ptychagnostus punctuosus* and *Lejopyge laevigata* Zones at Paibi (Peng and Robison, 2000). The *Glyptagnostus stolidotus* Zone overlies the *Lejopyge* zones in the lower part of the Chefu Formation at Wa'Ergang and Paibi. The *Glyptagnostus reticula-*

Table 3
Stable Isotope Data, Wa'ergang, China

Meters	^{13}C	^{18}O	Formation	Zone	Meters	^{13}C	^{18}O	Formation	Zone
137.20	0.63	−7.83	Huaqiao	not zoned	530.00	1.49	−10.48	Bitao	not zoned
147.00	0.38	−6.46	Huaqiao	*P. atavus*	540.00	2.67	−8.27	Bitao	not zoned
165.00	−0.28	−10.78	Huaqiao	*P. atavus*	550.00	1.60	−9.51	Bitao	not zoned
200.00	0.65	−7.96	Huaqiao	*P. atavus*	560.00	1.78	−9.52	Bitao	not zoned
210.00	1.82	−7.23	Huaqiao	*L. armata*	575.00	1.45	−9.77	Bitao	not zoned
219.55	0.19	−8.94	Huaqiao	*L. armata*	590.00	1.27	−10.03	Bitao	not zoned
266.00	1.08	−7.56	Huaqiao	*L. armata*	600.00	1.26	−10.02	Bitao	not zoned
274.00	0.79	−7.52	Huaqiao	*L. armata*	608.70	2.15	−7.53	Bitao	not zoned
280.35	0.69	−9.64	Huaqiao	*L. armata*	610.60	2.89	−8.74	Bitao	not zoned
282.00	0.69	−9.22	Chefu	*L. armata*	625.30	2.48	−8.00	Bitao	not zoned
283.00	1.70	−5.45	Chefu	*L. armata*	660.00	1.47	−10.18	Shenjiawan	not zoned
290.00	0.86	−8.61	Chefu	*L. armata*	697.85	2.66	−7.95	Shenjiawan	not zoned
300.20	1.63	−8.05	Chefu	*L. armata*	712.10	2.35	−7.80	Shenjiawan	not zoned
309.00	2.47	−8.06	Chefu	*L. armata*	721.00	0.88	−9.53	Shenjiawan	not zoned
320.30	1.88	−8.16	Chefu	*G. stolidotus*	735.00	1.90	−6.78	not described	not zoned
330.00	2.93	−8.31	Chefu	*G. stolidotus*	750.00	1.53	−8.35	not described	not zoned
340.00	3.28	−8.27	Chefu	*G. stolidotus*	760.00	2.36	−8.04	not described	not zoned
350.00	2.51	−8.84	Chefu	*G. reticulatus*	773.50	1.78	−9.67	not described	not zoned
361.00	3.28	−8.34	Chefu	not zoned	786.70	1.44	−9.72	not described	not zoned
369.75	5.03	−8.98	Bitao	not zoned	797.40	0.55	−9.41	not described	not zoned
380.10	4.40	−9.84	Bitao	not zoned	803.00	1.44	−9.60	not described	not zoned
390.00	4.23	−8.44	Bitao	not zoned	830.00	0.36	−9.18	not described	not zoned
400.00	4.38	−9.09	Bitao	not zoned	842.70	1.95	−9.31	not described	not zoned
409.70	3.76	−8.64	Bitao	not zoned	850.50	1.49	−9.41	not described	not zoned
411.00	3.16	−10.83	Bitao	not zoned	858.30	1.44	−9.72	not described	not zoned
420.00	2.96	−10.34	Bitao	not zoned	872.50	1.81	−9.02	not described	not zoned
430.00	4.70	−8.74	Bitao	not zoned	876.00	1.93	−10.11	not described	not zoned
440.00	4.21	−8.98	Bitao	not zoned	888.90	1.01	−10.54	not described	not zoned
450.00	4.60	−10.56	Bitao	not zoned	889.10	1.42	−9.94	not described	not zoned
460.00	3.67	−7.17	Bitao	not zoned	890.00	1.03	−9.96	not described	not zoned
470.00	4.28	−9.23	Bitao	not zoned	880.90	1.50	−9.16	not described	not zoned
480.00	4.53	−10.31	Bitao	not zoned	885.60	1.15	−9.88	not described	not zoned
490.00	4.22	−9.20	Bitao	not zoned	896.00	0.91	−9.97	not described	not zoned
501.00	3.15	−10.44	Bitao	not zoned	940.00	1.36	−9.46	not described	not zoned
509.00	3.78	−8.54	Bitao	not zoned	1000.00	1.94	−9.61	not described	not zoned
520.00	2.86	−10.41	Bitao	not zoned					

tus Zone is the youngest characterized agnostid zone and it is well represented in collections worldwide. Peng and Robison (2000) have proposed that the first appearance of *G. reticulatus* at Paibi be recognized as a potential Global Standard Stratotype-section and Point (GSSP). Zonally diagnostic trilobites younger than *G. reticulatus* are only represented at the Wa'Ergang section and include: *Irvingella*, *Rhaptagnostus*, *Westergaardites* and *Ivshinaspis* (Fig. 2). Sampling for carbon isotopes was continuous through the *P. atavus* to *G. stolidotus* zones at Paibi and Wa'Ergang, but only the Wa'Ergang section was sampled to capture the *G. reticulatus* Zone and higher parts of the Upper Cambrian.

2.3. Northwestern Queensland, Australia

The carbonates sampled in the Mt. Whelan core in Northwestern Queensland were deposited in an intracratonic basin formed during faulting of the Mount Isa block. Deposition in a deep water, stratified portion of the intracratonic basin is indicated by organic-rich, pyritic facies that show

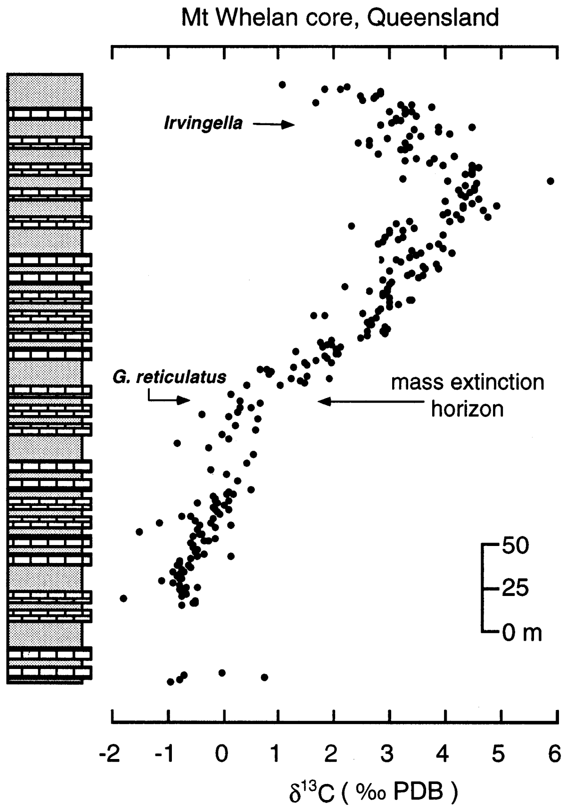

Fig. 3. Plots of $\delta^{13}C$ of limestones from the Mt. Whelan core in Queensland, Australia. First occurrence of cosmopolitan trilobite *Glyptagnostus reticulatus* is shown (Green and Balfe, 1980). Lithologies are fine-grained limestone and argillaceous limestone (solid pattern). The Mindyallan–Idamean stage boundary lies at the mass extinction horizon indicated by *G. reticulatus*.

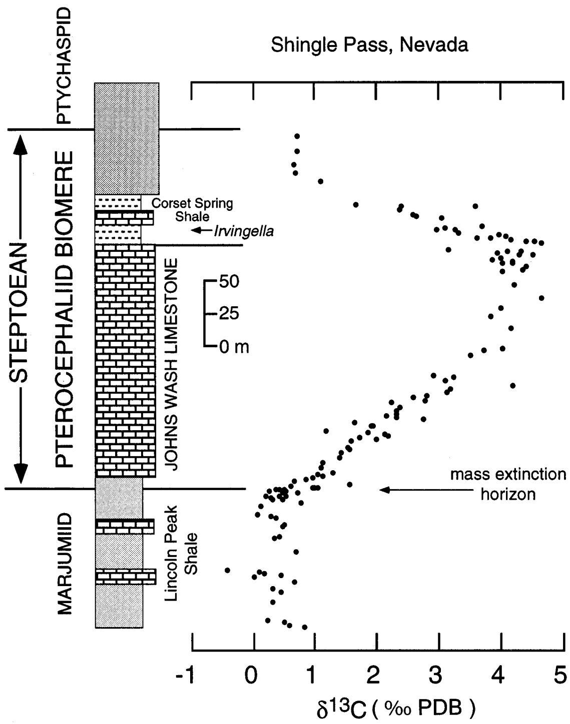

Fig. 4. The Marjumiid–Pterocephaliid biomere boundary (Marjuman–Steptoean stage boundary) is located to ±0.5 m (Thomas, 1993; Saltzman et al., 1998). *Irvingella angustilimbata* occurs ~10 m above the base of the Corset Spring Shale. Solid pattern is fine-grained limestone, block pattern is coarse-grained limestone and dashed pattern is shaly-limestone.

millimetre-scale laminations and contain in situ ammonium feldspars (Green and Balfe, 1980) indicative of a poorly oxygenated water mass. Though sparsely fossiliferous, the occurrences of *Glyptagnostus reticulatus* and *Irvingella* (Fig. 3) provide critical ties to the sections in China and Kazakhstan (Fig. 2).

2.4. East-central Nevada, USA

The Upper Cambrian mixed carbonate–clastic strata of the eastern Great Basin have been the subject of intensive study for over 50 years (Palmer; 1965; Osleger and Read, 1993; Saltzman et al., 1998; and references therein). Facies belts representing a vast carbonate platform extend for hundreds of kilometers from northeastern Utah into southeastern California. The Shingle Pass section in the southern Egan Range occurs towards the outer margin of this platform and has been studied in detail by Saltzman et al. (1998). Facies sampled for stable isotope analysis at Shingle Pass included a variety of shallow water carbonate environments: algal boundstone; oolitic grainstone; fenestral mudstones; and crinoidal packstones (Johns Wash Limestone) that are interbedded at the meter scale. Variable siliciclastic influx is recorded in the upper quarter of the section by the Corset Springs Shale (Fig. 4).

It is in the Great Basin where the SPICE excursion was first detected by Brasier (1993) within the biostratigraphic unit known as the Pterocephaliid biomere (Palmer, 1984). The

Pterocephaliid biomere is now considered the equivalent to the Steptoean Stage (Ludvigsen and Westrop, 1985; Palmer, 1998). At Shingle Pass, the base of the Steptoean Stage coincides with the first occurrence of *Coosella perplexa* (Thomas, 1993) near the top of the Lincoln Peak Shale. This fauna corresponds to the lowest occurrence of *Glyptagnostus reticulatus* in other sections in North America (Palmer, 1962) and is the basis for global correlation. *Irvingella* occurs near the middle of the Corset Springs Shale and provides a second key tie point with the sections in China, Kazakhstan and Australia.

3. Carbon isotope stratigraphy

3.1. Sample selection and methods

Bulk-rock samples were preferentially drilled from fine-grained lithologies, although the heterogeneity of carbonate facies within and between sections necessitated occasional sampling of coarser-grained lithologies (e.g. Johns Wash Limestone at Shingle Pass). Analytical work was carried out in stable isotope laboratories at the California Institute of Technology, Oxford University, University of California, Santa Cruz, and University of Michigan, using standard procedures. All values are reported relative to the PDB standard. Data from Kazakhstan and China are listed in Tables 1–3; data from Nevada are given in Saltzman et al. (1998).

3.2. $\delta^{13}C$ profiles and correlation of inflections in SPICE excursion

Middle to Late Cambrian $\delta^{13}C$ profiles can be correlated from Kazakhstan through China to Australia by plotting the occurrences of cosmopolitan trilobite taxa (Fig. 2 and 3). The SPICE excursion reaches peak values between the first occurrence of *Glyptagnostus reticulatus* and the first occurrence of *Irvingella* in all four sections.

In China, $\delta^{13}C$ values show small-scale fluctuations between 0 and +1.5‰ in the interval preceding the SPICE excursion (Fig. 2). $\delta^{13}C$ values then rise steeply near the first occurrence of *Glyptagnostus reticulatus* and peak at +5.0‰. Pre-excursion $\delta^{13}C$ values near +1.5‰ are reached just after the first occurrence of *Rhaptagnostus*. At the Wa'Ergang section (Table 3), heavy $\delta^{13}C$ values appear in the *Glyptagnostus stolidotus* Zone (Fig. 2), although we suspect that this reflects uncertainty in biostratigraphic resolution because elevated ratios do not appear in the *G. stolidotus* Zone in the better known section at Paibi (Table 2; Peng and Robison, 2000). In Kazakhstan, $\delta^{13}C$ values vary between −1.5 and +0.5‰, showing no clear trend throughout the pre-SPICE strata that include the *Ptychagnostus atavus* through *G. stolidotus* trilobite zones (Fig. 2; Table 2). $\delta^{13}C$ values then rise sharply above +1.5‰ at the first occurrence of *G. reticulatus* and peak at +4.8‰ just below the first occurrence of *Irvingella* (*Psuedagnostus curtare* Zone of Ergaliev, 1981). A steady decline in $\delta^{13}C$ reaches pre-excursion ratios mid-way through the local stratigraphic range of *Irvingella* (in the lower *Ivshinagnostus ivshini* Zone of Ergaliev; Table 2).

In Australia, $\delta^{13}C$ ratios rise steadily from near −1 to +1‰ in the interval preceding the SPICE excursion (Fig. 3). The marked rise in $\delta^{13}C$ to ratios above +5‰ begins at the level of *Glyptagnostus reticulatus*. In Nevada, $\delta^{13}C$ ratios are between 0 and +1‰ in the interval preceding the SPICE excursion (Fig. 4) and begin to rise at the first occurrence of *Coosella perplexa* (equivalent to the base of the *G. reticulatus* Zone). The peak above +5‰ occurs prior to the first occurrence of *Irvingella angustilimbata*.

4. Discussion

4.1. Connection with extinctions

The start of the SPICE excursion coincides with a worldwide mass extinction of trilobites at the base of the *Glyptagnostus reticulatus* Zone. In Australia, this extinction event was first recognized by Öpik (1966), who noted that none of the 80 species of trilobites then known from the preceding zone of *Glyptagnostus stolidotus* survived into the overlying *G. reticulatus* Zone. In North America, Palmer (1965) documented a drop in generic diversity of nearly 50% at the equivalent horizon. Öpik (1966) suggested an extraterrestrial cause (increase in solar luminosity) for this global mass extinction but this idea is untested; Orth et al. (1984) found no evidence (Ir enrichment) for bolide impact.

Throughout the Cambrian, it has been suggested that a permanent thermocline segregated provincial, warm-water, platform trilobites from their cool-water cosmopolitan counterparts (Cook and Taylor, 1975; Babcock, 1994). The latter were able to colonize the shallow, high-latitude, epicontinental seas of Avalonia and Baltica but are also found as invaders of tropical shelves during times of high sea level. So it is clear that the cool-water trilobites were able to migrate around the world beneath the thermocline. Stitt (1975) and Palmer (1984) noted that early Steptoean trilobites appear to have been adapted to cold waters typical of continental slope settings and suggested that the sub-Steptoean extinctions were caused by cooling resulting from ocean overturn. However, Pratt (1992, 1998) has documented a sub-Steptoean mass extinction of indigenous trilobites in a deep-ramp setting, which is inconsistent with Stitt's hypothesis.

The nature of the pre-SPICE killing mechanism is unknown. The connection between mass extinctions and positive isotope excursions at other times during the Phanerozoic suggests the possibility of a common cause. In the best-studied example, the C–T boundary, extinctions began soon after the onset of the $\delta^{13}C$ excursion and continued through its peak (Jarvis et al., 1988). In this case, the extinctions have been attributed to a disruption of the food chain that occurred because essential nutrients were depleted by the enhanced production that generated the positive excursion (Paul and Mitchell, 1994). Development of anoxia has also been proposed as a kill mechanism (Arthur et al., 1987). In contrast, the rise of the SPICE excursion was a time of faunal diversification, at least in Laurentia (Palmer, 1965, 1984; Rowell and Brady, 1976). These fundamental differences highlight the importance of further detailed studies of coupled extinctions and $\delta^{13}C$ excursions of this type.

4.2. *Models to explain $\delta^{13}C$ excursions*

Three models have been advanced to explain positive carbon isotope excursions. The oceanic anoxic events (OAE) model of Arthur et al. (1987) and the Monterey model of Vincent and Berger (1985) involve enhanced removal of organic matter during periods of high productivity and/or anoxia. The OAE model postulates increasing the burial fraction (f_{org},) of organic carbon relative to total carbon buried in sediments (Kump, 1991) while the Monterey model allows for an increase in total carbon buried during the $\delta^{13}C$ excursion. A third model — the weathering model — recently put forth in Kump et al. (1999) shifts the focus from changes in f_{org}, to changes in the isotopic composition of riverine runoff ($\delta^{13}C_{riv}$). These terms are related to the isotopic composition of marine carbonates ($\delta^{13}C_{carb}$) and the fractionation between carbonate and organic carbon ($\Delta^{13}C$) by the steady-state mass-balance equation (Kump, 1991; Kump et al., 1999):

$$f_{org} = \frac{\delta^{13}C_{carb} - \delta^{13}C_{riv}}{\Delta^{13}C} \quad (1)$$

Kump et al. (1999) attribute the positive carbon isotope excursion associated with the end-Ordovician glaciation to increases $\delta^{13}C_{riv}$ associated with weathering of carbonate platforms during sea level fall, whereas the two older ideas — OAE and the Monterey model — employ productivity-driven changes in the burial flux of organic carbon caused by nutrients delivered as a result of enhanced coastal upwelling [although see Paul and Mitchell (1994), for an alternative explanation for the C–T oceanic anoxic event that involves decreased productivity]. The OAE and the Monterey models require the formation of copious amounts of organic-rich (black) shales near sites of upwelling, where oxygen minimum zones intersect continental margins. All three models make testable predictions about fluctuations in sea level (high in the OAE model), changes in atmospheric pCO_2, and the rates of burial of organic matter during positive carbon isotope excursions (constant in the weathering model). Based on evidence for sea level fall and erosion of the carbonate platform during the time of the SPICE excursion in North America (*Dunderbergia* Zone in Osleger and Read, 1993; Saltzman et al., 1998; Glumac and Walker, 1998), SPICE appears to be a positive excursion similar to the Late Ordovician event of Kump et al. (1999). However, enhanced organic matter burial during the SPICE excursion seems likely (e.g. the organic-rich Alum Shale of Baltica), but can not yet be proven because black shales apparently spanned a considerable portion of the Late Cambrian (Thickpenny, 1987).

There is no unambiguous evidence for glaciation during the Late Cambrian, which highlights potential differences between the SPICE excursion and the larger +7‰ Late Ordovician and smaller +1‰ Miocene events. Though the SPICE may ultimately prove to display characteristics of both the Late Ordovician (enhanced carbonate weathering) and Miocene events (enhanced organic carbon burial), it is clearly distinct from the C–T event, which peaked with the warmest tropical SSTs (~33°C) and highest absolute sea level of the whole Cretaceous (Kolodny and Raab, 1988; Sahagian and Holland, 1991; Jenkyns et al., 1994).

General circulation models of Ordovician climate require higher levels of atmospheric CO_2 to compensate for reduced solar luminosity (~95% of present) 400–500 m.y. ago (Crowley and Baum, 1995; Gibbs et al., 1997). However, even with CO_2 set as high as 14 PAL, the north polar ocean remains colder than 0°C throughout the year. This effect should have been exacerbated by the ~8% faster rotation of the Earth (Jenkins et al., 1993; Williams, 1997), but it would also have been moderated by the low albedo of a largely landless northern hemisphere (Fig. 1). In such a world, the formation of perennial sea ice in the north polar ocean may have had dramatic effects on ocean circulation (Brenchley et al., 1994).

Thual and McWilliams (1992) and Saravanan and McWilliams (1995) have identified three stable equilibria obtained from idealized ocean models: TH — globally symmetric circulation, thermally driven by polar downwelling and equatorial upwelling; SA — globally symmetric circulation driven by downwelling from the cooler edges of mid-latitude salinity maxima and equatorial upwelling; PP — globally asymmetric circulation, thermally and salinity driven by downwelling at one pole and upwelling at the other (two possible steady states). Transitions from one state to another may be infrequent, even on geological timescales, and the consequences of a change of state are likely to be profound and long-lasting. For example, modeled hemispheric convection in the SA state has maximum flow rates two to three times less than those obtained under TH and PP conditions.

By analogy with other greenhouse times, it is assumed that for most of the Cambrian and Ordovician the oceans were operating in the SA state. We postulate a sudden transformation in oceanic circulation to a north-sinking PP state, perhaps triggered by the formation of sea ice in the north polar ocean, and reinforced by the retention of SA circulation in the land-rich southern hemisphere. Nutrients delivered to southern continental margins could have stimulated new production, some of which may be sequestered in widespread, organic-rich, black shales and limestones such as the Alum Shales (Baltica; Thickpenny, 1987) and Elliot Cove Formation (Avalonia; Hayes, 1948). The precise timing and rates of organic matter burial related to these events are not well known, although they may ultimately prove to be the tangible legacy of the SPICE excursion.

Simulations of the SPICE excursion using the two-box model of Junge et al. (1975) and Brocker and Peng (1982) as developed by Kump (1991) show that an instantaneous doubling of the fraction of organic versus carbonate carbon sequestered in the global oceans could generate the SPICE excursion in less than a million years [using values for Δ, and the fluxes and their isotopic compositions in Kump (1991)]. A slower rise to peak values, consistent with an estimated duration of ~4 m.y. (Saltzman et al., 1998), implies some kind of positive feedback to increase progressively the burial fraction of organic versus carbonate carbon (f_{org}) from ca. 0.2 to ca. 0.35. This positive feedback could have been supplied by CO_2 drawdown which induced global cooling and eventually resulted in a sea level minimum at the peak of the excursion (Sauk II–Sauk III hiatus), which also should have increased $\delta^{13}C_{riv}$. Much of the required modest fall in sea level (<25 m) may be attributed to thermal contraction of the deep ocean coupled with increased groundwater storage in terrestrial reservoirs.

5. Conclusions

Our measurements of $\delta^{13}C$ from limestones of Late Cambrian age in Laurentia, Gondwana and periGondwanan terranes [south China (?), Kazakhstan] reveal, in unprecedented detail, one of the largest known carbon isotope excursions of the whole Phanerozoic. Positive excursions of this scale (+5‰) are sufficiently uncommon to be readily identified in noisy or sparsely sampled datasets [SPICE was discovered with only four datapoints; Brasier (1993)]. The survival of the primary (heavy) carbon isotope signature, even in dolomitized or highly altered rocks such as those hosting Mississippi Valley-type (MVT) ore deposits (He, 1995), is a clear indication that the SPICE excursion will be a valuable tool for precise regional and intercratonic correlation of Late Cambrian events, even in deformed terranes. As it begins at or near the base of the zone of *Glyptagnostus reticulatus*, the SPICE excursion may be used globally to locate one of the primary subdivisions of the Cambrian System (Palmer, 1998; Peng and Robison, 2000) in unfossiliferous carbonate or carbonaceous sequences.

Acknowledgements

The authors would like to thank the staff of the Exploration Data Centre, Zillmere, Queensland, for assistance with sampling the Mt. Whelan core; J.H. Shergold for suggesting the Mt. Whelan section; M.N. Rees and L.E. Babcock for information about the Chinese sections sampled by them; J.L. Kirschvink, B. Tursunov and A. Bekleuv for help in sampling the Kyrshabakty locality; M.J. Vendrasco and R. Hill for help in the field; L. Wingate, R. Selnikov and Y. Silberstein for analytical assistance; and J.C. McWilliams, J.D. Neelin, and R.C. Thomas for discussion and advice. Funds for this work were provided by UCLA; the American Association of Petroleum Geologists; the Geological Society of America; the Institute for Cambrian Studies; and the Sir Charles Clore Fellowship program of the Weizmann Institute of Science. The authors especially thank A.R. Palmer and an anonymous reviewer for through and thoughtful reviews; IGPP Publication No. 5181.

References

Arthur, M.A., Schlanger, S.O., Jenkyns, H.C., 1987. The Cenomanian–Turonian oceanic anoxic event, II. Palaeoceanographic controls on organic-matter production and preservation. Geological Society, London, Special Publication 26, 401–420.

Babcock, L.E., 1994. Biogeography and biofacies patterns of Middle Cambrian polymeroid trilobites from North Greenland: palaeogeographic and palaeo-oceanographic implications. Groenlands Geologiske Undersoegelse 169, 129–147.

Brasier, M.D., 1993. Towards a carbon isotope stratigraphy of the Cambrian System: potential of the Great Basin succession. Geological Society, London, Special Publication 70, 341–350.

Brenchley, P.J., Marshall, J.D., Carden, G.A.F., Robertson, D.B.R., Long, D.G.F., Meidla, T., Hints, L., Anderson, T.F., 1994. Bathymetric and isotopic evidence for a short-lived Late Ordovician glaciation in a greenhouse period. Geology 22, 295–298.

Brocker, W.S., Peng, T., 1982. Tracers in the Sea: Palisades. Columbia University, New York.

Cook, H.E., Taylor, M.E., 1975. Early Paleozoic continental margin sedimentation, trilobite biofacies, and the thermocline, western United States. Geology 3, 559–562.

Cook, H.E., Taylor, M.E., Zhemchuzhnikov, S.V., Apollonov, M.K., Ergaliev, G.K., Sargaskaev, Z.S., Dubinina, S.V., 1991. . In: Cooper, J.D., Stevens, C.H. (Eds.), Paleozoic paleogeography of the western United States — II. SEPM Pacific Section, Los Angeles, pp. 847–872.

Crowley, T.J., Baum, S.K., 1995. Reconciling Late Ordovician (440 Ma) glaciation with very high (14X) CO_2 levels. Journal of Geophysical Research 100, 1093–1101.

Ergaliev, G.K., 1981. Upper Cambrian biostratigraphy of the Kyrshabakty section, Maly aratau, southern Kazakhstan. U.S. Geological Survey Open-File Report 81-743, 82–88.

Gibbs, M.T., Barron, E.J., Kump, L.R., 1997. An atmospheric pCO_2 threshold for glaciation in the Late Ordovician. Geology 25, 447–450.

Glumac, B., Walker, K.R., 1998. A Late Cambrian positive carbon-isotope excursion in the southern Appalachians: relation to biostratigraphy, sequence stratigraphy, environments of deposition, and diagenesis. Journal of Sedimentary Research 68, 1212–1222.

Green, P.M., Balfe, P.E., 1980. Stratigraphic drilling report — GSQ Mt Whelan 1 and 2. Queensland Government Mining Journal 81, 162–178.

Grotzinger, J.P., Bowring, S.A., Saylor, B.Z., Kaufman, A.J., 1995. Biostratigraphic and geochronologic constraints on early animal evolution. Science 270, 598–604.

Hayes, A.O., 1948. Geology of the area between Bonavitsa and

Trinity bays, eastern Newfoundland. Newfoundland Geological Survey Bulletin 32, 1–34.

He, Z., 1995. Sedimentary facies and variation of stable isotope composition of Upper Cambrian to Lower Ordovician strata in southern Missouri: implications for the origin of MVT deposits and the geochemical and hydrological features of regional ore-forming fluids. Unpublished Ph.D. Dissertation, University of Missouri, Rolla.

Jarvis, I., Carson, G.A., Cooper, M.K.E., Hart, M.B., Leary, P.N., Tocher, B.A., Horne, D., Rosenfeld, A., 1988. Microfossil assemblages and the Cenomanian–Turonian (late Cretaceous) oceanic anoxic event. Cretaceous Research 9, 3–103.

Jenkins, G.S., Marshall, H.G., Kuhn, W.R., 1993. Precambrian climate: the effects of land area and Earth's rotation rate. Journal of Geophysical Research 98, 8785–8791.

Jenkyns, H.C., Gale, A.S., Corfield, R.M., 1994. Carbon- and oxygen-isotope stratigraphy of the English Chalk and Italian Scaglia and its palaeoclimatic significance. Geological Magazine 131, 1–34.

Joachimski, M.M., Buggisch, W., 1993. Anoxic events in the late Frasnian — causes of the Frasnian–Famennian faunal crisis? Geology 21, 675–678.

Junge, C.E., Schidlowski, M., Eichmann, R., Pietrek, H., 1975. Model calculations for the terrestrial carbon cycle: carbon isotope geochemistry and evolution of photosynthetic oxygen. Journal of Geophysical Research 80, 4542–4552.

Kolodny, Y., Raab, M., 1988. Oxygen isotopes in phosphatic fish remains from Israel: Paleothermometry of tropical Cretaceous and Tertiary shelf waters. Palaeogeography, Palaeoclimatology, Palaeoecology 64, 59–67.

Kump, L.R., 1991. Interpreting carbon-isotope excursions: Strangelove oceans. Geology 111, 299–302.

Kump, L.R., Arthur, M.A., Patzkowsky, M.E., Gibbs, M.T., Pinkus, D.S., Sheehan, P.M., 1999. A weathering hypothesis for glaciation at high atmospheric pCO2 during the Late Ordovician. Palaeogeography, Palaeoclimatology, Palaeoecology 152, 173–187.

Ludvigsen, R., Westrop, S.R., 1985. Three new Upper Cambrian stages for North America. Geology 13, 139–143.

Öpik, A.A., 1966. The early Upper Cambrian crisis and its correlation. Journal and Proceedings of the Royal Society of New South Wales 100, 9–14.

Orth, C.J., Knight, J.D., Gilmore, L.R., Palmer, A.R., 1984. A search for iridium abundance anomalies at two Late Cambrian biomere boundaries in western Utah. Science 223, 163–165.

Osleger, D.A., Read, J.F., 1993. Comparative analysis of methods used to define eustatic variations in outcrop: Late Cambrian interbasinal sequence development. American Journal of Science 293, 157–216.

Palmer, A.R., 1962. *Glyptagnostus* and associated trilobites in the United States. U.S. Geological Survey Professional Paper 374-F, 1–49.

Palmer, A.R., 1965. Trilobites of the Late Cambrian Pterocephaliid Biomere in the Great Basin, United States. U.S. Geological Survey Professional Paper 493, 1–105.

Palmer, A.R., 1984. The biomere problem: evolution of an idea. Journal of Paleontology 58, 599–611.

Palmer, A.R., 1998. A proposed nomenclature for stages and series for the Cambrian of Laurentia. Canadian Journal of Earth Sciences 35, 323–328.

Paul, C.R.C., Mitchell, S.F., 1994. Is famine a common factor in marine mass extinctions? Geology 22, 679–682.

Peng, S., 1992. Upper Cambrian biostratigraphy and trilobite faunas of the Cili-Taoyuan area, northwestern Hunan, China. Memoir of the Association Australasian Palaeontologists 13, 1–119.

Peng, S., Robison, R.A., 2000. In: Agnostoid Biostratigraphy Across the Middle–Upper Cambrian Boundary in China. Paleontological Society Memoir. Paleontological Society, pp. 1–333.

Pratt, B.R., 1992. Trilobites of the Marjuman and Steptoean stages (Upper Cambrian), Rabbitkettle Formation, southern Mackenzie Mountains, northwest Canada. Palaeontographica Canadiana 9, 1–179.

Pratt, B.R., 1998. Probable predation on Upper Cambrian trilobites and its relevance for the extinction of soft-bodied Burgess Shale-type animals. Lethaia 31, 73–88.

Rowell, A.J., Brady, M.J., 1976. Brachiopods and Biomeres. Brigham Young University Geology Studies 23, 165–180.

Rowell, A.J., Robison, R.A., Strickland, D.K., 1982. Aspects of Cambrian agnostoid phylogeny and chronocorrelation. Journal of Paleontology 56, 161–182.

Sahagian, D.L., Holland, S.M., 1991. Eustatic sea-level curve based on a stable frame of reference: preliminary results. Geology 19, 1209–1212.

Saltzman, M.R., Runnegar, B., Lohmann, K.C., 1998. Carbon isotope stratigraphy of Upper Cambrian (Steptoean Stage) sequences of the eastern Great Basin: record of a global oceanographic event. Geological Society of America Bulletin 110, 285–297.

Saravanan, R., McWilliams, J.C., 1995. Multiple equilibria, natural variability, and climate transitions in an idealized ocean-atmosphere model. Journal of Climate 8, 2296–2323.

Scholle, P.A., Arthur, M.A., 1980. Carbon isotope fluctuations in Cretaceous pelagic limestones: potential stratigraphic and petroleum exploration tool. American Association of Petroleum Geologists Bulletin 64, 67–87.

Scotese, C.R., McKerrow, W.S., 1990. Revised World maps and introduction. Geological Society, London, Memoir 12, 1–21.

Stitt, J.H., 1975. Adaptive radiation, trilobite paleoecology and extinction, Ptychaspid Biomere, Late Cambrian of Oklahoma. Fossils and Strata 4, 381–390.

Thickpenny, A., 1987. Palaeo-oceanography and depositional environment of the Scandanavian Alum Shales: sedimentological and geochemical evidence. In: Legett, J.K., Zuffa, G.G. (Eds.), Marine Clastic Sedimentology. Graham and Trotman, London, pp. 156–171.

Thomas, R.C., 1993. The Marjumiid–Pterocephaliid (Upper Cambrian) mass extinction event in the western United States. Unpublished Ph.D. Dissertation, University of Washington, Seattle.

Thual, O., McWilliams, J.C., 1992. The catastrophe structure of thermohaline convection in a two-dimensional fluid model and a comparison with low-order box models. Geophysical and Astrophysical Fluid Dynamics 64, 67–95.

Tucker, R.D., McKerrow, W.S., 1995. Early Paleozoic chronology: a review in light of new U–Pb zircon ages from Newfoundland and Britain. Canadian Journal of Earth Sciences 32, 368–379.

Underwood, C.J., Crowley, S.F., Marshall, J.D., Brenchley, P.J., 1997. High-resolution carbon isotope stratigraphy of the basal Silurian stratotype (Dob's Linn, Scotland) and its global correlation. Journal of the Geological Society, London 154, 709–718.

Vincent, E., Berger, W.H., 1985. Carbon dioxide and polar cooling in the Miocene: The Monterey hypothesis. In: Sundquist, E.T., Broecker, W.S. (Eds.), The Carbon Cycle and Atmospheric CO_2: Natural Variations Archean to Present. American Geophysical Union, Washington, DC, pp. 455–468.

Walcott, C.D., 1913. The Cambrian faunas of China. Carnegie Institute of Washington Publication 54, 1–375.

Wang, K., Geldsetzer, H.H.J., Goodfellow, W.D., Krouse, H.R., 1996. Carbon and sulfur isotope anomalies across the Frasnian–Famennian extinction boundary, Alberta, Canada. Geology 24, 187–191.

Williams, G.E., 1997. Precambrian length of day and the validity of tidal rhythmite paleotidal values. Geophysical Research Letters 24, 421–424.